Matter

CellPress

Article

Additive Manufacturing of Ductile, Ultrastrong Polymer-Derived Nanoceramics

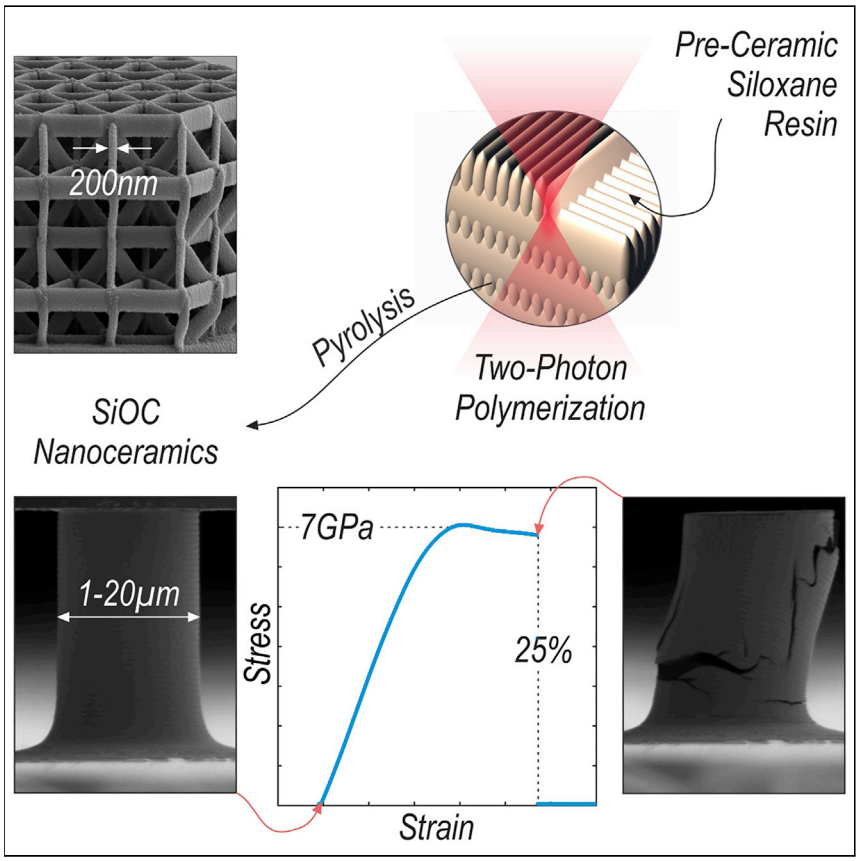

Ductile high-strength ceramics would be ideal for many structural applications; however, they have been neither demonstrated at dimensions much above the nanoscale nor shown to be manufacturable with application-relevant processes. Here, we present a robust route to additively manufacture ductile, ultrastrong silicon oxycarbide nanoceramics via two-photon polymerization of a preceramic resin and subsequent pyrolysis. We measure plastic deformability with strains up to 25% and strengths >7 GPa for 20-μm specimens, opening up potential for fabrication of mesoscale ductile ceramic components.

Jens Bauer, Cameron Crook, Anna Guell Izard, Zak C. Eckel, Nicolas Ruvalcaba, Tobias A. Schaedler, Lorenzo Valdevit

valdevit@uci.edu

HIGHLIGHTS

SiOC is the strongest, stiffest, most resilient two-photon polymerizable material

SiOC pillars up to 20 μm in diameter display plastic deformation and strength >7 GPa

200-nm feature sizes can be printed, with only 30% shrinkage upon pyrolysis

4 **Demonstrate**
Proof-of-concept of performance with intended application/response

Bauer et al., Matter *1*, 1–10
December 4, 2019
https://doi.org/10.1016/j.matt.2019.09.009

Please cite this article in press as: Bauer et al., Additive Manufacturing of Ductile, Ultrastrong Polymer-Derived Nanoceramics, Matter (2019), https://doi.org/10.1016/j.matt.2019.09.009

Matter

CellPress

Article

Additive Manufacturing of Ductile, Ultrastrong Polymer-Derived Nanoceramics

Jens Bauer,[1] Cameron Crook,[2] Anna Guell Izard,[1] Zak C. Eckel,[3] Nicolas Ruvalcaba,[1] Tobias A. Schaedler,[3] and Lorenzo Valdevit[1,2,4,*]

SUMMARY

Ceramics would be ideal engineering materials if their brittleness and scattered fracture strength could be overcome. While ductility and extraordinary strength have been reported at the nanoscale, they both rapidly disappear when samples reach micrometer dimensions; furthermore, manufacturing is limited to elaborate approaches, which are purely scientific in nature. Here, we present a robust route to additively manufacture ductile, ultrastrong silicon oxycarbide (SiOC) via two-photon polymerization direct laser writing (TPP-DLW) of a preceramic resin and subsequent pyrolysis. We 3D-print micrometer-size pillars and architected materials with feature sizes down to ~200 nm and characterize them under uniaxial compression. Independent of size, SiOC micropillars consistently deform plastically with strains up to 25% and strengths >7 GPa, across the entire range of examined diameters (1–20 μm). Our findings demonstrate straightforward fabrication of ductile, ultrastrong ceramics at previously unprecedented scales, potentially enabling manufacturing of engineering systems up to tens of millimeters in size.

INTRODUCTION

Ceramics are known to become ductile at room temperature below dimensions of typically tens of nanometers to a few micrometers.[1–5] If ductility in ceramics became accessible to engineering systems, it would entail a long-desired major technological leap forward. Possessing high stiffness and intrinsic strength, high thermal and chemical resistance, and low density, ceramics could be ideal materials for many structural engineering applications, ranging from automotive to aerospace and energy systems. However, their brittle nature often prevents practical applications.

To date, fabrication of ductile nanoceramics has mostly been limited to elaborate and geometrically constrained purely scientific approaches, such as focused ion beam (FIB) milling of thin films. In general, ceramics are difficult to process, with brittleness deriving from processing-induced porosity, cracks, and inhomogeneities.[6] Recently, UV-curable preceramic resins have been demonstrated to additively manufacture[7–9] complex-shaped parts that were subsequently pyrolyzed into low-flaw-population amorphous silicon oxycarbide (SiOC). However, existing data on mechanical properties is limited to specimens with characteristic length scales of millimeters, with failure still governed by brittle fracture. From these data, fracture strengths of the constituent SiOC on the order of 300–600 MPa[7,9] can be estimated.

As the highest-resolution fully three-dimensional (3D) additive manufacturing technology, two-photon polymerization direct laser writing (TPP-DLW)[10,11] with

Progress and Potential

Ductile high-strength ceramics exist at extremely small scales, but have been neither demonstrated at dimensions much above the nanoscale nor shown to be manufacturable with application-relevant processes. At larger scales, processing-induced flaws cause the characteristic ceramic brittleness. If ductility in ceramics became accessible to engineering systems, it would entail a long-desired technological leap forward. We show that two-photon polymerization 3D-printing with a preceramic resin followed by pyrolysis is a robust route to the manufacture of ultrastrong ductile ceramics, at dimensions far beyond the nanoscale. We print architectures with feature sizes down to 200 nm and monolithic pillars with diameters up to 20 μm. Pillar compression consistently shows plasticity with strains up to 25% and strengths >7 GPa. With the straightforward printability demonstrated herein, millimeter-size engineering systems, composed of microscale ductile, ultrastrong ceramic features, may now be realized.

Please cite this article in press as: Bauer et al., Additive Manufacturing of Ductile, Ultrastrong Polymer-Derived Nanoceramics, Matter (2019), https://doi.org/10.1016/j.matt.2019.09.009

preceramic resins may provide a pathway to fabrication of high-performance, ductile nanoceramics. Although limited to polymers, a few industrial applications of TPP-DLW for micrometer- and millimeter-size engineering devices have been proposed over the past few years.[12–16] So far, the only mechanically characterized TPP-DLW-derived ceramic is pyrolytic glassy carbon.[17–19] Pyrolysis of carefully designed polymeric microstructures has been shown to create exceptionally strong glassy carbon nanostructures.[17] However, brittle deformation behavior with inherently scattered, size-, geometry-, and process-sensitive properties, as well as shrinkage up to 90% upon pyrolysis, are generally reported.[17–20] Scattered plastic deformability was observed in pillar compression experiments,[18] but the effect rapidly disappears when pillar diameters reach the micrometer scale and the mechanical properties degrade. Applicability of high-strength TPP-DLW-derived glassy carbon appears limited to architected materials with characteristic features at the smallest scales.

In this paper, we report the additive manufacturing of ultrastrong yet ductile SiOC ceramics via TPP-DLW of a preceramic photo resin and subsequent pyrolysis. We show that this SiOC formulation is the strongest, stiffest, and most resilient two-photon polymerizable material reported to date. We present high-quality 3D SiOC nanoarchitectures with feature sizes down to ~200 nm and shrinkages upon pyrolysis of only ~30%. Based on compression of monolithic pillars, we find strengths of 7 GPa, which is an up to 20-fold increase from previously reported additively manufactured SiOC;[7,9] yet we report ductile deformation behavior with failure strains of up to 25%. Remarkably, these properties are very consistent across the entire range of examined specimens, up to diameters of 20 μm, with typical variabilities of only ±3%. To date, ductile and ultrastrong ceramics have been neither demonstrated at dimensions much above the nanoscale nor shown to be manufacturable with any application-relevant fabrication approach. Our findings demonstrate accessibility of ductility and ultrahigh strength far beyond the nanoscale, as well as straightforward printability via TPP-DLW, with significant implications for the design and fabrication of micro- and mesoscale engineering systems.

RESULTS

TPP-DLW with a siloxane resin system enables synthesis of high-quality 3D nano- and microarchitected SiOC structures. Figure 1 shows representative octet nanolattices, woodpile photonic crystals, and monolithic micropillars before and after pyrolysis. The printability and the resulting feature quality and resolution of the polymerized structures match that of state-of-the-art TPP resins.[10] Pyrolysis at 1,000°C yields undistorted ceramic SiOC structures with feature sizes down to ~200 nm (Figure 1B). Upon pyrolysis, structures linearly shrink by approximately 30%, as reported for larger-scale additively manufactured SiOC.[7,8]

Uniaxial compression of TPP-DLW-derived SiOC (TPP-SiOC) micropillars with diameters between 1 and 20 μm consistently shows ductile deformation behavior with failure strains up to 25% and ultrahigh strengths on the order of the theoretical limit (~E/10) (Figure 2A). With yield strengths (σ_y) of 5.0 ± 0.3 GPa and fracture strengths (σ_f) of 6.9 ± 0.3 GPa, the material is up to 20 times stronger than any previously reported larger-scale SiOC[7,9] additively manufactured from similar resin systems, as well as bulk SiOC[21] (Figure 2B). The corresponding plastic strains of typically 7%–15% clearly show substantial ductility, independent on the specimen size. Young's moduli (E) of 66 ± 2 GPa are approximately double those of TPP-derived glassy carbon[18] and on the order of previously reported values for SiOC.[3,21] As characteristic for ductile amorphous ceramics,[3–5] we find a bulging deformation mechanism without detectable shear bands,

[1]Mechanical and Aerospace Engineering Department, University of California, Irvine, CA 92697, USA

[2]Materials Science and Engineering Department, University of California, Irvine, CA 92697, USA

[3]HRL Laboratories Limited Liability Company, Malibu, CA 90265, USA

[4]Lead Contact

*Correspondence: valdevit@uci.edu

https://doi.org/10.1016/j.matt.2019.09.009

Please cite this article in press as: Bauer et al., Additive Manufacturing of Ductile, Ultrastrong Polymer-Derived Nanoceramics, Matter (2019), https://doi.org/10.1016/j.matt.2019.09.009

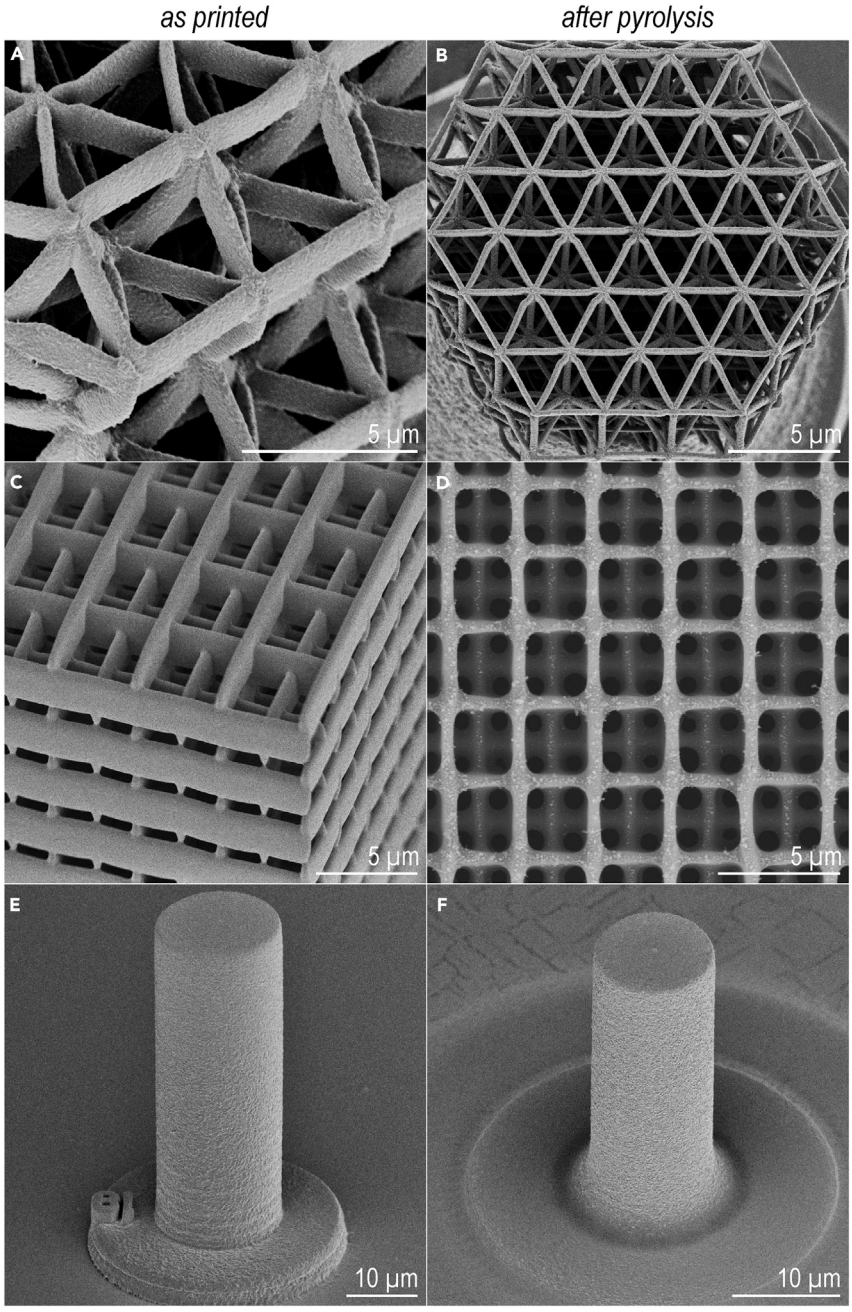

Figure 1. Additive Manufacturing of SiOC Nanoceramics via Two-Photon Polymerization Direct Laser Writing and Pyrolysis

As-printed polymeric and pyrolyzed SiOC octet nanolattice (A and B), woodpile photonic crystal (C and D), and micropillar (E and F).

followed by longitudinal crack nucleation, which can lead to vertical splitting. Figures 2C–2L show different-sized specimens before testing and at failure. With decreasing specimen size, the top surfaces of the pillars become increasingly conical-shaped due to manufacturing constraints (Figures 2C and 2D); for specimens with diameters below 2 μm, this geometric defect causes early crack nucleation and reduced strengths and Young's moduli; these defected tests have not been considered in the averages presented above.

Please cite this article in press as: Bauer et al., Additive Manufacturing of Ductile, Ultrastrong Polymer-Derived Nanoceramics, Matter (2019), https://doi.org/10.1016/j.matt.2019.09.009

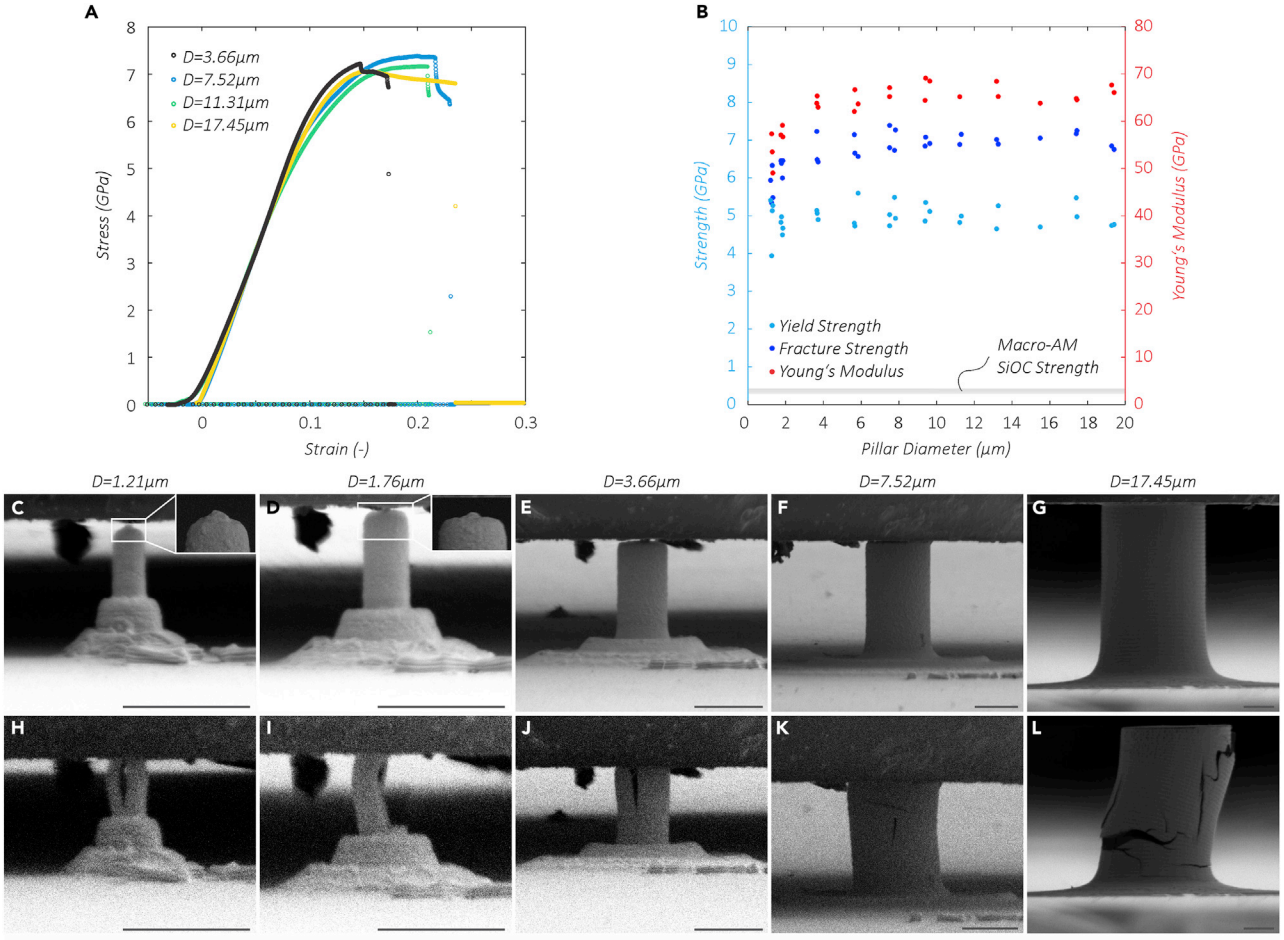

Figure 2. Mechanical Characterization of SiOC Micropillars

(A) Stress-strain curves showing ductile deformation behavior independent of the pillar diameter (D).

(B–L) Ultrahigh yield strengths (σ_y), fracture strengths (σ_f), and Young's moduli (E) as a function of D (B). SEM images of different-sized pillars (C–G) before testing and (H–L) at failure. Scale bars, 5 μm.

Transmission electron microscopy (TEM) of the TPP-SiOC reveals a completely amorphous microstructure, free of any detectable pores. Figure 3 shows bright- and dark-field scanning TEM images as well as a selected area diffraction pattern of a sample extracted from the center plane of a 12-μm-wide and 36-μm-high micropillar. Via energy-dispersive X-ray spectroscopy (EDS), we find a uniform distribution of silicon, carbon, oxygen, and sulfur (Figure 3D) with a composition of 20.2 atom % Si, 33.5 atom % C, 44.8 atom % O, and 1.6 atom % S, which is comparable with previously reported polymer-derived SiOC.[7]

SiOC octet nanolattices are the stiffest and strongest mechanical metamaterials reported to date (Figure 4).[22] Under uniaxial compression, we measure effective stiffnesses of 1–17 GPa and strengths of 40–860 MPa at 9%–40% relative density ($\bar{\rho}$), i.e., the volume fraction of the solid constituent material. Elastic-plastic behavior with failure strains up to 8% is observed. With the significantly higher constituent stiffness of SiOC compared with materials such as glassy carbon, the specific stiffness of the SiOC nanolattices, i.e., the ratio of stiffness to density, more than tripled with respect to the most advanced nano- and microarchitected materials.[22] Compared with some architected materials, topological effects may in addition to

Please cite this article in press as: Bauer et al., Additive Manufacturing of Ductile, Ultrastrong Polymer-Derived Nanoceramics, Matter (2019), https://doi.org/10.1016/j.matt.2019.09.009

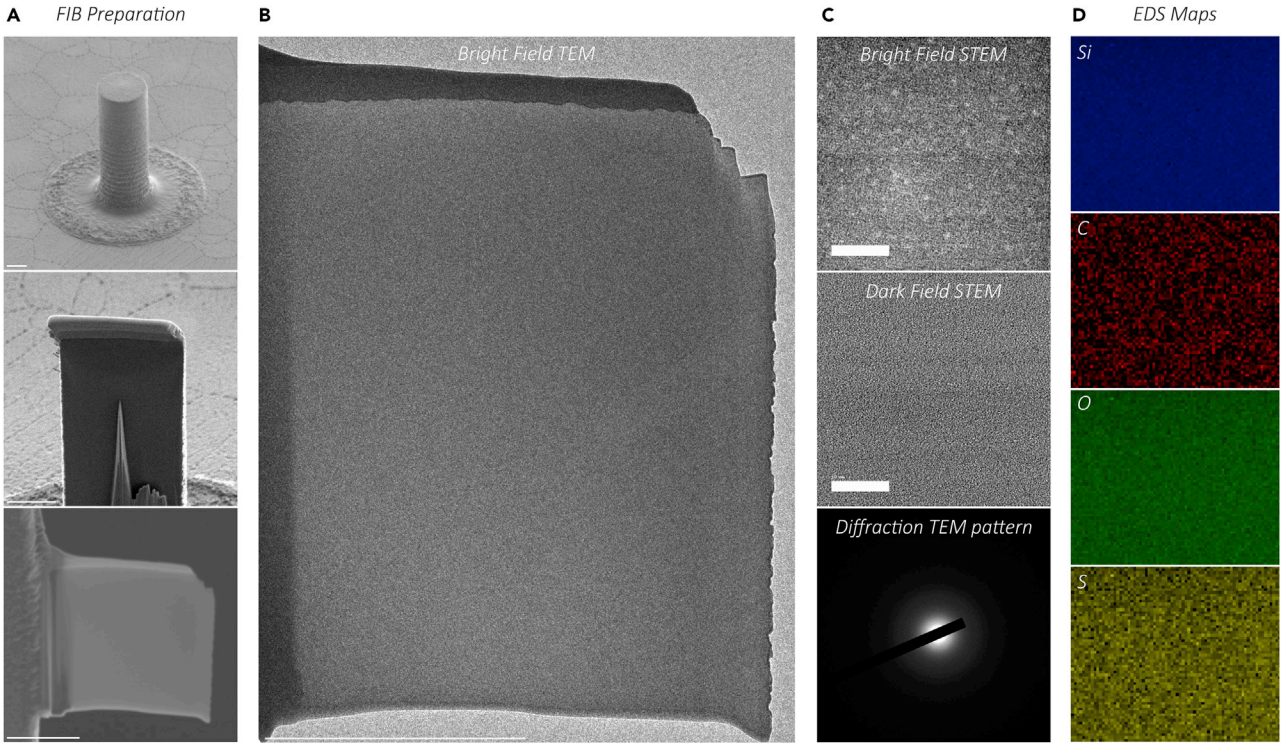

Figure 3. Microstructural Characterization via Transmission Electron Microscopy

(A and B) Sample extraction from the center plane of a micropillar using FIB milling (A) and (B) TEM image. Scale bars, 5 μm.

(C) Bright- and dark-field high-resolution scanning TEM (STEM) images and selected area diffraction TEM patterns showing no porosity and amorphous structure. Scale bars, 10 nm.

(D) Energy-dispersive X-ray spectroscopy (EDS) maps showing uniform distribution of silicon, carbon, oxygen, and sulfur.

the constituent SiOC contribute to the found stiffness gain, here all octet lattices were tested along the stiffest direction (<111>). Specific strengths, i.e., the ratio of strength to density, are on a par with those of previously reported glassy carbon nanolattices[17,19] and substantially exceed those of any other cellular material. The effective stiffness of cellular materials (E_{eff}) can be approximated by the first-order scaling law $E_{eff} \propto E_s \bar{\rho}^{n_1}$, with the Young's modulus of the constituent solid material (E_s), the relative density ($\bar{\rho}$), and the scaling exponent (n_1). Similarly, the effective strength (σ_{eff}) can be modeled as $\sigma_{eff} \propto \sigma_s \bar{\rho}^{n_2}$,[23] with the yielding or fracture strength of the constituent solid material (σ_s) and the scaling exponent (n_2). Ideal stretching-dominated architectures have scaling exponents n_1 and n_2 equal to 1.[24] The scaling behavior of many reported micro- and nanoarchitected materials is substantially worse than predicted by the ideal models, due to imperfections or hollow node design.[22] Here we found linear scaling of the stiffness (n_1 = 0.98) and close to linear scaling of the strength (n_2 = 1.37) above $\bar{\rho} \approx 20\%$. In the range of ~20% relative density, the governing failure mechanism changes from material fracture to architectural instability (Figure 4A), as characteristic for ultrastrong nanolattices where extreme ratios of constituent material strength-to-Young's modulus ($\sigma_s/E_s \approx 1/10$) cause buckling at much higher $\bar{\rho}$ than for large-scale architected materials.[22,25] Correspondingly, the scaling exponents increase to n_1 = 1.68 and n_2 = 2.21; n_2 is in good agreement with the theory of lattice failure by elastic buckling.[25] The simultaneous increase in n_1 is known to relate to the complexity of extracting stiffness data[26] before premature buckling and is consistent with the scaling of many architected materials shown in Figure 4C.

Please cite this article in press as: Bauer et al., Additive Manufacturing of Ductile, Ultrastrong Polymer-Derived Nanoceramics, Matter (2019), https://doi.org/10.1016/j.matt.2019.09.009

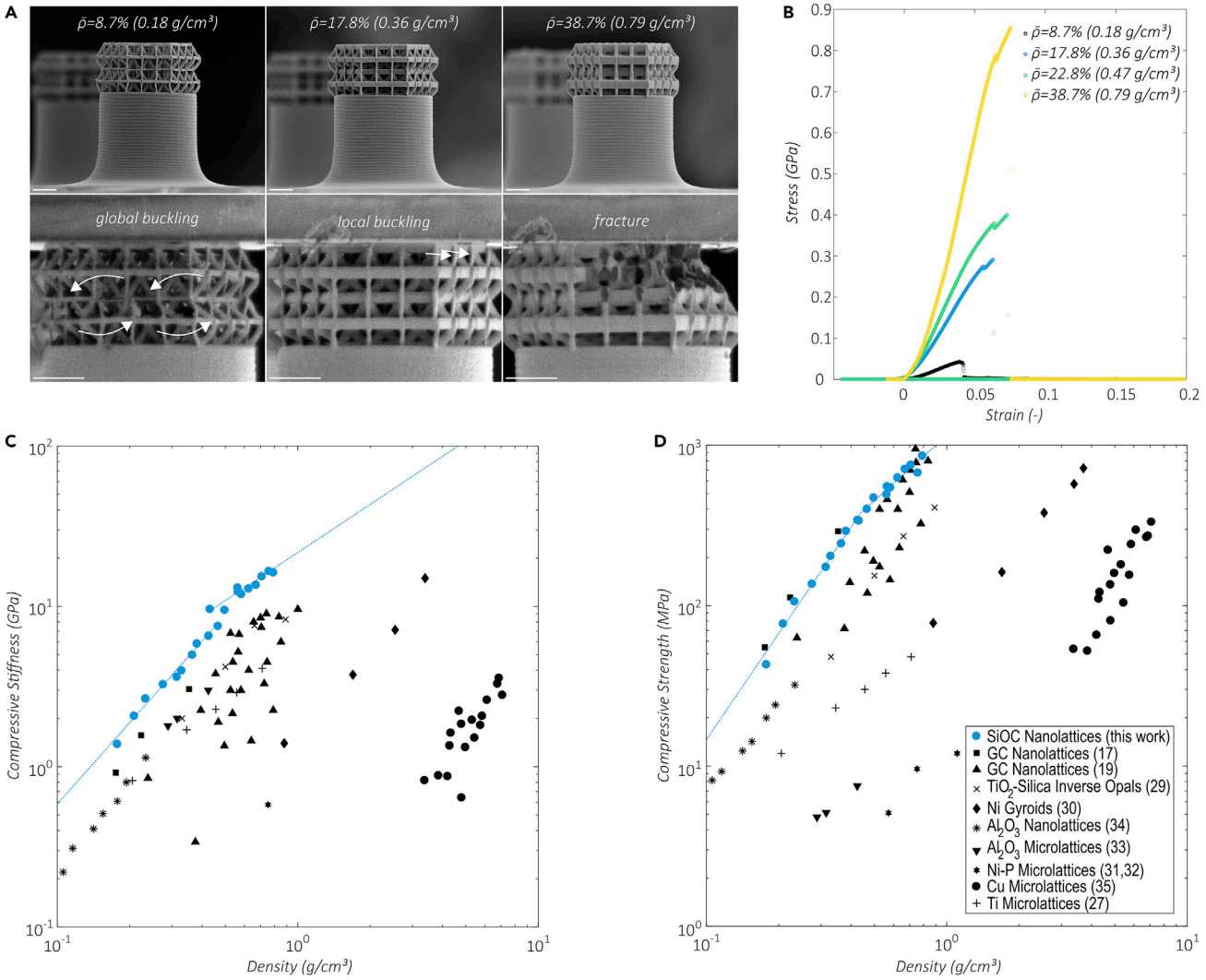

Figure 4. Mechanical Characterization of SiOC Nanolattices

(A) SiOC nanolattice before mechanical characterization (top) and at the moment of failure (bottom). Scale bars, 5 μm.

(B–D) Compressive stress-strain curves showing elastic-plastic behavior at higher densities (B). Material property charts showing the (C) stiffness and (D) strength of SiOC nanolattices compared with other mechanical metamaterials.[17,19,27–35]

DISCUSSION

Plasticity under compression in amorphous materials such as silica glass is governed by two major mechanisms: (1) volume-conserving shear flow[36] through localized bond-switching events, and (2) volumetric strain by irreversible densification[37] in the case of a very open structure. The structure of amorphous SiOC may be approximated as a continuous random network of tetrahedral SiO_4 units, just as in silica glass, with some replacements of O atoms by C atoms.[3] Silica glass has been shown to predominantly experience volume-conserving shear flow.[5] With a Poisson's ratio of 0.21,[38] typical transverse strains at failure in the range of ~5% may be expected for the SiOC samples under pure volume-conserving shear flow.[5] These strains are in good agreement with scanning electron microscopy (SEM) measured values over ~3%, suggesting that volume-conserving shear flow is, as in silica glass, dominating the plastic response of TPP-SiOC, with only minor contributions from densification.

Please cite this article in press as: Bauer et al., Additive Manufacturing of Ductile, Ultrastrong Polymer-Derived Nanoceramics, Matter (2019), https://doi.org/10.1016/j.matt.2019.09.009

Neither shear flow nor densification are considered intrinsically size dependent, although they both require very high activation stresses (here ~5 GPa), which in practice are unapproachable due to the much lower fracture strength. Fracture strength highly depends on the processing-sensitive flaw population[6] and is well known to increase with decreasing dimensions.[39] Previously reported plasticity under compression of amorphous ceramics[3–5,18] is limited to specimen diameters <5 μm. In this work we find no detectable flaws in our SiOC samples (Figure 3), resulting in fracture stresses on the order of the theoretical strength (~E/10) and, hence, plastic deformability across the entire size range of examined samples.

The size-independent low-flaw population of the presented TPP-derived SiOC, which enables ductility, ultrahigh strength, and the remarkable scalability of both, is attributed to two key mechanisms. (1) Compared with larger-scale additively manufactured SiOC, the substantially increased resolution of TPP-DLW may drastically reduce the flaw population in a printed part, independently of its overall dimensions. The ~200-nm-size TPP-DLW build volume that is polymerized at one time reduces surface roughness of printed components from tens of micrometers to a few nanometers, thus alleviating surface roughness-induced crack nucleation. Simultaneously, the short diffusion paths during printing may result in a lower inner-material flaw population than in stereolithography or self-propagating polymer waveguide processing, whereby much larger material volumes are polymerized at once.[22] (2) In contrast to TPP-derived ceramics such as pyrolytic glassy carbon, TPP-SiOC is rather insensitive to size-to-volume and surface-to-volume effects. Pyrolysis of polymers into glassy carbon involves the decomposition and outgassing of the majority of the polymeric material, as reflected in the extreme shrinkages of up to 90%. With increasing size, average diffusion paths for molecules to exit the material become longer and may cause void formation and degradation of the mechanical properties. In contrast, most of the presented preceramic polymer transforms into SiOC, correlating with the fairly low shrinkage of only ~30%. Additionally, the fully amorphous microstructure of TPP-SiOC results in uniform mechanical properties with low variability. In contrast, surface-induced graphitization in pyrolytic glassy carbon causes different ratios of crystalline-to-amorphous domains[40] depending on the specimen size and shape, contributing to a pronounced size effect and scatter in the mechanical properties.

Preceramic resins such as the presented siloxane resin system have the potential to replace current state-of-the-art acrylate resins. Up to now, industrial adoption of TPP-DLW has been partly hindered by the weak mechanical properties of commonly used polymers. While pyrolysis of acrylate resins has previously been employed to create mechanically resilient glassy carbon, its application relevance is to date somewhat limited: typical Young's moduli and strengths of TPP-DLW-derived glassy carbon are half of those of the SiOC presented here, and inherently scattered;[17,18] shrinkage is up to 3-fold higher; and plastic deformability is reportedly limited to very small-scale samples with feature sizes up to ~2 μm.[18] The high quality of the TPP-SiOC structures demonstrated in this study, down to ~200 nm feature size, further highlights the potential of preceramic resins to compete with established polymeric resins in terms of printability and precision.

If carefully designed, engineering systems may be able to exploit the beneficial properties of TPP-SiOC, with overall component dimensions at the millimeter scale. The recently demonstrated ability to manufacture centimeter-size complex parts[41] without sacrificing submicrometer accuracy may increase scalability even further. The potential existence of a ductile-to-brittle transition for larger-size TPP-SiOC remains to be investigated. However, most application-ready TPP-DLW-fabricated components consist of

Please cite this article in press as: Bauer et al., Additive Manufacturing of Ductile, Ultrastrong Polymer-Derived Nanoceramics, Matter (2019), https://doi.org/10.1016/j.matt.2019.09.009

subcomponents with feature size at the micrometer scale,[12–16] a dimensional range in which we still find ductility and ultrahigh strength. To maintain plastic deformability in a complex part, it will be critical to avoid surface-induced stress concentrations. The fracture strength and, therefore, plastic deformability are inherently sensitive to stress concentrations, as the imperfect conical-shaped pillars in Figures 2C and 2D indicate. Likewise, the sharp notches at the nodes of the nanolattices limit their macroscopic plastic deformability by inducing premature tensile failure at the nodes.[42] Particularly under tensile loading, designing a component that guarantees activation of plastic flow mechanisms before fracture is a substantial challenge.

Conclusion

Our results demonstrate that TPP-DLW with the siloxane resin system investigated here is a robust route to manufacture ultrastrong yet ductile ceramics, at scales far beyond the nanoscale. Previously, no application-relevant manufacturing approach has demonstrated fabrication of ductile ceramics, much less at dimensions of tens of micrometers. At the same time, we demonstrate that this process is suitable for fabrication of nanoarchitected metamaterials with excellent specific stiffness and strength. Beyond the superior mechanical properties reported herein, the exceptional thermal stability, combined with irradiation, oxidation, and creep resistance, makes TPP-SiOC an ideal material for functional elements, such as high-temperature thermophotovoltaic emitters.[43]

EXPERIMENTAL PROCEDURES

Fabrication

All specimens were manufactured via TPP-DLW from a UV-curable siloxane resin system, formulated by mixing (mercaptopropyl)methylsiloxane (Gelest) and vinylmethoxysiloxane (Gelest) at a 1:1 molar ratio of thiol/vinyl groups, a UV free radical photoinitiator Irgacure 819 (BASF) at 0.25 wt %, and a free radical scavenger as an inhibitor at 0.2%. TPP-DLW was performed using a Photonic Professional GT (Nanoscribe) DLW system equipped with a Plan-Apochromat 63× 1.4 Oil DIC M27 (Carl Zeiss) objective and a FemtoFiber pro NIR (Toptica Photonics) laser, with a center wavelength of 780 nm, a pulse width of ~100 fs, and a repetition rate of 80 MHz. Specimens were printed on silicon substrates. After TPP-DLW, samples were submerged in toluene for 40 min to dissolve uncured photoresist, followed by two 10-min-long isopropanol baths for further cleaning. Subsequently specimens were dried using an Autosamdri-931 (Tousimis Research) critical point dryer. The polymeric specimens were then pyrolyzed to SiOC in a vacuum tube furnace. A heating profile of 1°C/min to 1,000°C, 60 min hold at 1,000°C, and cooling to room temperature at 3°C/min was used. Micropillars with nominal diameters of 2–30 μm and height-to-diameter ratios of 2 and 3 were printed in a layer-by-layer fashion with a writing speed (v) of 5,000 μm/s, a laser average power (P) of 50 mW, and a hatching distance and slicing distance of 0.1 μm and 0.2 μm between adjacent lines and planes, respectively. Octet lattices had 5-μm size unit cells and were printed from 3D single-line trajectories with v = 10 μm/s. Relative densities between 8% and 40% were realized by varying P between 16 and 36 mW. During pyrolysis, all specimens underwent linear isotropic shrinkage of approximately 30%. SiOC octet lattices had elliptical strut cross-sections with widths and heights of 200–600 nm and 500–1,720 nm, respectively.

Mechanical Testing

Specimen dimensions were optically measured using an FEI Magellan 400XHR (Thermo Fisher Scientific) scanning electron microscope. To determine the mechanical properties of the TPP-DLW-derived SiOC, we performed uniaxial *in situ* compression experiments at a constant strain rate of 0.003 s^{-1} inside an FEI Quanta 3D FEG

Please cite this article in press as: Bauer et al., Additive Manufacturing of Ductile, Ultrastrong Polymer-Derived Nanoceramics, Matter (2019), https://doi.org/10.1016/j.matt.2019.09.009

(Thermo Fisher Scientific) dual-beam (SEM/FIB), with an Alemnis Nanoindenter (Alemnis) equipped with a flat punch diamond tip, 100 μm in diameter. Load-displacement curves were recorded, and displacement correction was performed for equipment and substrate compliances by an in-house digital image correlation algorithm, whereby specimen top and bottom were tracked. Applying the measured dimensions, engineering stress and strain were determined. E was extracted as the maximum slope of the linear elastic regime and σ_y as the 0.2% yield offset of the corresponding stress-strain curve. σ_f was the maximum engineering stress. Relative and effective densities of nanolattices were determined by computer-aided design models and SEM-measured dimensions. The density of monolithic SiOC[7] was 2.05 g/cm^3.

Materials Characterization

Scanning TEM and qualitative EDS were performed with a 300-kV JEM-ARM300F Grand ARM (JEOL) with spherical aberration correction. Selected area diffraction TEM patterns were collected from the specimen interior using a JEM-2100F (JEOL) operated at 200 kV using a 30-cm camera length. The lamella was extracted from the vertical center plane of a 12-μm wide pillar by FIB milling with an FEI Quanta 3D FEG (Thermo Fisher Scientific) dual-beam SEM/FIB. Quantitative EDS characterization was performed using an FEI Quanta 3D FEG dual-beam SEM/FIB at 10 kV equipped with an Oxford X-MAX 50 silicon 50-mm^2 drift detector (SDD). EDS spectra were collected from the top surfaces of 19.4-μm diameter pillars. Quantification of spectra was performed using INCA (Oxford Instruments).

ACKNOWLEDGMENTS

This research was supported by a NASA Early Stage Innovation program, award #80NSSC18K0259. J.B. gratefully acknowledges partial financial support from the Deutsche Forschungsgemeinschaft, grant BA 5778/1-1. SEM and TEM imaging and *in situ* mechanical testing were performed at the UC Irvine Materials Research Institute. Use of the FEI Quanta 3D FEG dual-beam (SEM/FIB) is funded in part by the National Science Foundation Center for Chemistry at the Space-Time Limit (CHE-0802913).

AUTHOR CONTRIBUTIONS

J.B., T.A.S., and L.V. conceived the research; Z.C.E. developed the resin mixture; J.B., C.C., A.G.I., and N.R. manufactured specimens and performed mechanical experiments; C.C. conducted TEM measurements; C.C. and J.B. performed EDS measurements; J.B. analyzed data; J.B., C.C., A.G.I., Z.C.E., T.A.S., and L.V. interpreted results; J.B. wrote the manuscript.

DECLARATION OF INTERESTS

The authors declare no conflicts of interest. HRL Laboratories has been awarded patent numbers US 10,196,464 and US 10,221,284.

Received: May 25, 2019
Revised: August 10, 2019
Accepted: September 9, 2019
Published: October 9, 2019

REFERENCES

1. Luo, J., Wang, J., Bitzek, E., Huang, J.Y., Zheng, H., Tong, L., Yang, Q., Li, J., and Mao, S.X. (2016). Size-dependent brittle-to-ductile transition in silica glass nanofibers. Nano Lett. *16*, 105–113.

2. Östlund, F., Rzepiejewska-Malyska, K., Leifer, K., Hale, L.M., Tang, Y., Ballarini, R., Gerberich, W.W., and Michler, J. (2009). Brittle-to-ductile transition in uniaxial compression of silicon pillars at room temperature. Adv. Funct. Mater. *19*, 2439–2444.

3. Ming, K., Gu, C., Su, Q., Wang, Y., Zare, A., Lucca, D.A., Nastasi, M., and

Wang, J. (2019). Strength and plasticity of amorphous silicon oxycarbide. J. Nucl. Mater. *516*, 289–296.

4. Lacroix, R., Kermouche, G., Teisseire, J., and Barthel, E. (2012). Plastic deformation and residual stresses in amorphous silica pillars under uniaxial loading. Acta Mater. *60*, 5555–5566.

5. Kermouche, G., Guillonneau, G., Michler, J., Teisseire, J., and Barthel, E. (2016). Perfectly plastic flow in silica glass. Acta Mater. *114*, 146–153.

6. Kurkjian, C.R., Gupta, P.K., and Brow, R.K. (2010). The strength of silicate glasses: what do we know, what do we need to know? Int. J. Appl. Glass Sci. *1*, 27–37.

7. Eckel, Z.C., Zhou, C., Martin, J.H., Jacobsen, A.J., Carter, W.B., and Schaedler, T.A. (2016). Additive manufacturing of polymer-derived ceramics. Science *351*, 58–62.

8. Hundley, J.M., Eckel, Z.C., Schueller, E., Cante, K., Biesboer, S.M., Yahata, B.D., and Schaedler, T.A. (2017). Geometric characterization of additively manufactured polymer derived ceramics. Addit. Manuf. *18*, 95–102.

9. Cui, H., Hensleigh, R., Chen, H., and Zheng, X. (2018). Additive manufacturing and size-dependent mechanical properties of three-dimensional microarchitected, high-temperature ceramic metamaterials. J. Mater. Res. *33*, 360–371.

10. Baldacchini, T. (2015). Three-Dimensional Microfabrication Using Two-Photon Polymerization, First Edition (Elsevier).

11. Hohmann, J.K., Renner, M., Waller, E.H., and von Freymann, G. (2015). Three-dimensional μ-printing: an enabling technology. Adv. Opt. Mater. *3*, 1488–1507.

12. Thiele, S., Arzenbacher, K., Gissibl, T., Giessen, H., and Herkommer, A.M. (2017). 3D-printed eagle eye: compound microlens system for foveated imaging. Sci. Adv. *3*, e1602655.

13. Nelson, G., Kirian, R.A., Weierstall, U., Zatsepin, N.A., Faragó, T., Baumbach, T., Wilde, F., Niesler, F.B., Zimmer, B., Ishigami, I., et al. (2016). Three-dimensional-printed gas dynamic virtual nozzles for x-ray laser sample delivery. Opt. Express *24*, 11515.

14. Rad, Z.F., Nordon, R.E., Anthony, C.J., Bilston, L., Prewett, P.D., Arns, J.Y., Arns, C.H., Zhang, L., and Davies, G.J. (2017). High-fidelity replication of thermoplastic microneedles with open microfluidic channels. Microsyst. Nanoeng. *3*, 17034.

15. Lissandrello, C.A., Gillis, W.F., Shen, J., Pearre, B.W., Vitale, F., Pasquali, M., Holinski, B.J., Chew, D.J., White, A.E., and Gardner, T.J. (2017). A micro-scale printable nanoclip for electrical stimulation and recording in small nerves. J. Neural Eng. *14*, 036006.

16. Di Giacomo, R., Krödel, S., Maresca, B., Benzoni, P., Rusconi, R., Stocker, R., and Daraio, C. (2017). Deployable micro-traps to sequester motile bacteria. Sci. Rep. *7*, 45897.

17. Bauer, J., Schroer, A., Schwaiger, R., and Kraft, O. (2016). Approaching theoretical strength in glassy carbon nanolattices. Nat. Mater. *15*, 438–443.

18. Albiez, A., and Schwaiger, R. (2019). Size effect on the strength and deformation behavior of glassy carbon nanopillars. MRS Adv. *4*, 133–138.

19. Zhang, X., Vyatskikh, A., Gao, H., Greer, J.R., and Li, X. (2019). Lightweight, flaw-tolerant, and ultrastrong nanoarchitected carbon. Proc. Natl. Acad. Sci. U S A *116*, 6665–6672.

20. Lim, Y., Heo, J., Madou, M., and Shin, H. (2013). Monolithic carbon structures including suspended single nanowires and nanomeshes as a sensor platform. Nanoscale Res. Lett. *8*, 492.

21. Renlund, G.M., Prochazka, S., and Doremus, R.H. (1991). Silicon oxycarbide glasses: Part II. Structure and properties. J. Mater. Res. *6*, 2723–2734.

22. Bauer, J., Meza, L.R., Schaedler, T.A., Schwaiger, R., Zheng, X., and Valdevit, L. (2017). Nanolattices: an emerging class of mechanical metamaterials. Adv. Mater. *29*, 1701850.

23. Gibson, L.J., and Ashby, M.F. (2001). Cellular Solids: Structure and Properties, Second Edition (Cambridge Univ. Pr.).

24. Deshpande, V.S., Ashby, M.F., and Fleck, N.A. (2001). Foam topology: bending versus stretching dominated architectures. Acta Mater. *49*, 1035–1040.

25. Deshpande, V.S., Fleck, N.A., and Ashby, M.F. (2001). Effective properties of the octet-truss lattice material. J. Mech. Phys. Sol. *49*, 1747–1769.

26. Salari-Sharif, L., and Valdevit, L. (2014). Accurate stiffness measurement of ultralight hollow metallic microlattices by laser vibrometry. Exp. Mech. *54*, 1491–1495.

27. Dong, L., Deshpande, V.S., and Wadley, H.N.G. (2015). Mechanical response of Ti-6Al-4V octet-truss lattice structures. Int. J. Solids Struct. *60*, 107–124.

28. do Rosário, J.J., Lilleodden, E.T., Waleczek, M., Kubrin, R., Petrov, A.Y., Dyachenko, P.N., Sabisch, J.E.B., Nielsch, K., Huber, N., Eich, M., and Schneider, G.A. (2015). Self-assembled ultra high strength, ultra stiff mechanical metamaterials based on inverse opals. Adv. Eng. Mater. *17*, 1420–1424.

29. do Rosário, J.J., Berger, J.B., Lilleodden, E.T., McMeeking, R.M., and Schneider, G.A. (2016). The stiffness and strength of metamaterials based on the inverse opal architecture. Extrem. Mech. Lett. *12*, 86–96.

30. Khaderi, S.N., Scherer, M.R.J., Hall, C.E., Steiner, U., Ramamurty, U., Fleck, N.A., and Deshpande, V.S. (2016). The indentation response of nickel nano double gyroid lattices. Extrem. Mech. Lett. *10*, 15–23.

31. Schaedler, T.A., Jacobsen, A.J., Torrents, A., Sorensen, A.E., Lian, J., Greer, J.R., Valdevit, L., and Carter, W.B. (2011). Ultralight metallic microlattices. Science *334*, 962–965.

32. Torrents, A., Schaedler, T.A., Jacobsen, A.J., Carter, W.B., and Valdevit, L. (2012). Characterization of nickel-based microlattice materials with structural hierarchy from the nanometer to the millimeter scale. Acta Mater. *60*, 3511–3523.

33. Zheng, X., Lee, H., Weisgraber, T.H., Shusteff, M., DeOtte, J., Duoss, E.B., Kuntz, J.D., Biener, M.M., Ge, Q., Jackson, J.A., et al. (2014). Ultralight, ultrastiff mechanical metamaterials. Science *344*, 1373–1377.

34. Meza, L.R., Das, S., and Greer, J.R. (2014). Strong, lightweight, and recoverable three-dimensional ceramic nanolattices. Science *345*, 1322–1326.

35. Gu, X.W., and Greer, J.R. (2015). Ultra-strong architected Cu meso-lattices. Extrem. Mech. Lett. *2*, 7–14.

36. Marsh, D.M., and Cottrell, A.H. (1964). Plastic flow in glass. Proc. R. Soc. Lond. Ser. A Math. Phys. Sci. *279*, 420–435.

37. Ernsberger, F.M. (1968). Role of densification in deformation of glasses under point loading. J. Am. Ceram. Soc. *51*, 545–547.

38. Du, P., Wang, X., Lin, I.-K., and Zhang, X. (2012). Effects of composition and thermal annealing on the mechanical properties of silicon oxycarbide films. Sensors Actuators A Phys. *176*, 90–98.

39. AA, G. (1921). The phenomena of rupture and flow in solids. Philos. Trans. R. Soc. Lond. A *221*, 163–198.

40. Ji, Y., Li, C., Wang, G., Koo, J., Ge, S., Li, B., Jiang, J., Herzberg, B., Klein, T., Chen, S., Sokolov, J.C., and Rafailovich, M.H. (2008). Confinement-induced super strong PS/MWNT composite nanofibers. Europhys. Lett. *84*, 56002.

41. Jonušauskas, L., Gailevičius, D., Rekštytė, S., Baldacchini, T., Juodkazis, S., and Malinauskas, M. (2019). Mesoscale laser 3D printing. Opt. Express *27*, 15205.

42. Bauer, J., Schroer, A., Schwaiger, R., and Kraft, O. (2016). The impact of size and loading direction on the strength of architected lattice materials. Adv. Eng. Mater. *18*, 1537–1543.

43. Nagpal, P., Han, S.E., Stein, A., and Norris, D.J. (2008). Efficient low-temperature thermophotovoltaic emitters from metallic photonic crystals. Nano Lett. *8*, 3238–3243.